Journal of Radioanalytical and Nuclear Chemistry (2020) 324:813–822
https://doi.org/10.1007/s10967-020-07111-x

Adsorption performance of U(VI) by amidoxime-based activated carbon

Peng Liu[1] · Qiang Yu[1] · Yun Xue[1] · Jiaqi Chen[1] · Fuqiu Ma[1]

Received: 29 December 2019 / Published online: 1 April 2020

Abstract
We present a simple strategy for preparing amidoxime modified activated carbon. The composition and morphology of the materials have been confirmed via powder XRD, BET, TGA, SEM and FT-IR studies. Batch adsorption experiment were exploited to explore adsorption performance of U(VI) by amidoxime-based activated carbon. The adsorption capacity of activated carbon was significantly improved after the modification by amidoxime, the amidoxime-based activated carbon was a possible adsorbent for adsorbing U(VI). This study reveals that with a facile synthesis and low-cost, amidoxime-based activated carbon can be regarded as a promising material for uranium-containing wastewater treatment.

Keywords Amidoxime · Activated carbon · Adsorption · Uranium-containing wastewater treatment

Introduction

With the shortage of fossil fuels, a new energy source that can replace the fossil fuels is needed urgently [1]. Nuclear power perceived a new energy option. At the same time, a plenty of long-lived radionuclides inevitably was accompanying with the development of nuclear industry [2]. Uranium has been widely used in many fields as a crucial radionuclide [3]. However, numerous radioactive daughter products of uranium are likely to cause a harmful effect on biosphere and human health in the process of exploitation and application [4–6]. Therefore, it is pressing to find a lowcost and eco-friendly method to treat uranium-containing wastewater.

Currently, many reserve approaches, such as chemical precipitation, photocatalytic degradation, electrodeposition, evaporation, adsorption, membrane separation, and other approaches, have been applied to treat the uranium-containing wastewater [7, 8]. However, most of these techniques for treating waste water are either too expensive or too ineffective. Currently, adsorption is taken into account of a promising treatment method on account of its simple operation and low-costing [9–11]. A variety of materials were widely studied for the removal of uranium from aqueous solutions [12]. Among multifarious adsorbents, activated carbon attracted much interest and were trusted to be an efficient adsorbent because of its good performance on the removal of uranium [13]. However, the missing of functional groups and the selectivity of activated carbon restricted its adsorption capacity [14]. Therefore, numerous functional groups such as benzoylthiourea [15], diarylazobisphenol [16], and polyethyleneimine [17] were selected to modify activated carbon by different technique for improving the adsorption performance of U(VI). Because of its great affinity to U(VI), adsorbents with amidoxime (AO) functional groups became the most protential materials in the field of uranium recovery from seawater [18]. In this work, activated carbon was direct modified by the prepared amidoxime polyacrylonitrile solution, as thus, the operation was simple and the production of intermediates was reduced.

The amidoxime-base activated carbon was accomplished, the influence of ambient condition and the mechanism of U(VI) adsorption was investigated in this work. Experimental results showed that amidoxime-base activated carbon can be regarded as a prospective adsorbent for the adsorption of U(VI) from uranium-containing wastewater.

✉ Fuqiu Ma
mafuqiu@hrbeu.edu.cn

[1] Harbin Engineering University, College of Nuclear Science and Technology, Harbin 150001, China

Materials and methods

Materials

All of the chemicals were analytical grade and dissolved with deionized water. U(VI) stock solution was made from $UO_2(NO_3)2 \cdot 6H_2O$. Arsenazo-III (Aladdin, China) solution was prepared by dissolving 1 g Arsenazo-III in 1000 mL of deionized water. Activated carbon particle was purchased from Tianjin Fuchen Chemicals, China. Polyacrylonitrile power was purchased from Daqing Petrochemical Acrylic Plant, China. Dimethyl sulfoxide (DMSO) and polyvinylpyrrolidone (PVP) were purchased from Shanghai Houcheng Chemicals. All reagents were analytically pure and used as received without further treatment.

Adsorbent preparation

Amidoxime-base activated carbon was prepared according to the under-mentioned procedure. 4.0 g of polyacrylonitrile power was dissolved in 200 mL of dimethyl sulfoxide (DMSO). After stirred for 1 day, 8.0 g of hydroxylamine hydrochloride was added to the solution. Then the mixture was stirred for 5 day at room temperature. 2 g of polyvinylpyrrolidone (PVP) and activated carbon were dispersed into the mixture. Then the homogeneous solution was coated to activated carbon by sol–gel method. Finally, the amidoxime-functionalized artificial activated carbon product was washed with ethyl alcohol and Milli-Q water 3 times and dried at 45 °C for 1 day [19].

Batch experiment

Calculated amounts of $NaNO_3$ solution, amidoxime-based activated carbon, uranium solution and deionized water were spiked into 50 mL polyethylene centrifuge tubes. HNO_3 or NaOH solution was added to adjust pH. The adsorbent and U(VI) solution were placed into a conical flask in an gas bath thermostatic oscillator (NKSY-200B, Shanghai Sukun, China) for 3 days. After 3 days, the samples were centrifuged and the supernatant was measured via Arsenazo-III spectrophotometric method [20]. The absorbance of uranium(VI)–Arsenazo-III complex was measured by a UV-1801 spectrophotometer (Beijing Rayleigh Analytical Instrument Co. Ltd., China) at 652 nm. Based on the experiment, the adsorption efficiency and capacity of U(VI) on amidoxime-based activated carbon was calculated as follows:

$$\eta = \frac{(C_0 - C_1)}{C_0} \times 100\% \quad (1)$$

$$q_e = \frac{(C_0 - C_1)}{m} \times V \quad (2)$$

where C_0 and C_1 are the initial and final concentration of U(VI), respectively; while m is the mass of amidoxime-based activated carbon.

Effect of initial pH

The pH of the solution was adjusted to the desired value (2.5–9.0) by adding NaOH or HNO_3. 0.11 g of absorbent, 3 mL of 0.1 mol/L $NaNO_3$, 12 mL of 100 mg/L U(VI) solution and 15 mL of deionized water were placed in a 50 mL polyethylene centrifuge tubes with continuously shaking at 298 K. The concentration of U(VI) before and after adsorption was determined.

Effect of time

The pH of the U(VI) solution was adjusted to the value of 5.0. 6 mL of 100 mg/L solution was 0.11 g of absorbent, 3 mL of 0.1 mol/L $NaNO_3$ and 15 mL of deionized water were placed in a 50 mL polyethylene centrifuge tubes, pH of the mixed solution was adjusted to the value of 5.0. Take the time of mix the solution with U(VI) solution as the initial time. The sample were shaking continuously at 298 K, take out the sample after the scheduled time, the supernatant was filtered out with the filter membrane at once to determine the concentration of U(VI) and thus to plot the amount adsorbed versus time.

Effect of temperature

The effect of temperature was carried out at 298, 308, 318, 328 and 338 K using various initial U(VI) concentrations (1–250 mg/L) at pH 5.0. The concentration of U(VI) before and after adsorption was determined.

Effect of adsorbent dosage

The effect of adsorbent dosage was carried out at 298 K using various adsorbent dosage (0.02–7 g/L) at pH 5.0. The concentration of U(VI) before and after adsorption was determined.

Characterization

The prepared amidoxime-based activated carbon was characterized using several techniques. Elemental analysis were obtained on an elementar vario MACRO cube. Fourier transform infrared spectroscopy (FT-IR) was obtained on a Nicolet Nexus 670 spectrometer using the standard KBr disk method. X-ray diffraction (XRD) measurements were

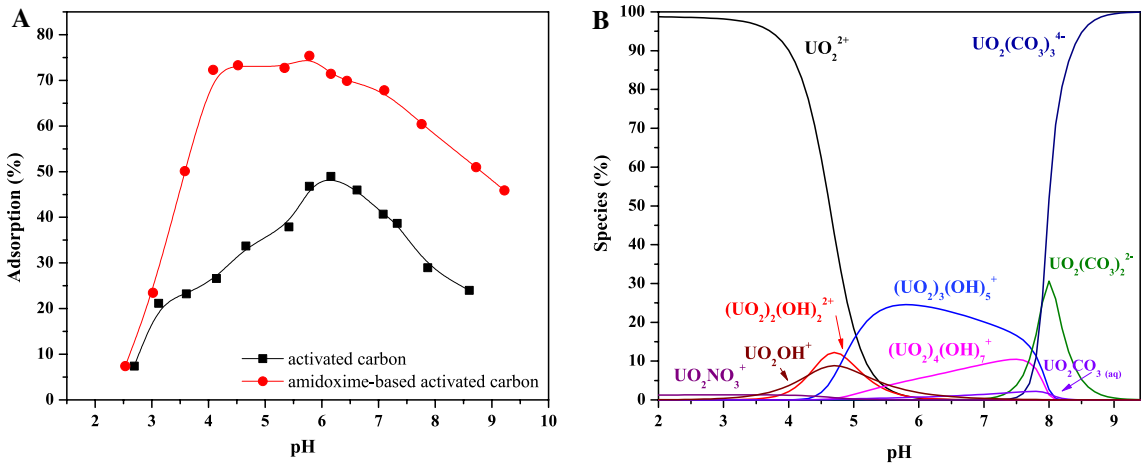

Fig. 1 Effect of pH on the U(VI) adsorption onto amidoxime-based activated carbon (**a**); relative species distribution of U(VI) in the presence of CO_2 (**b**). $m/V = 3.6$ g/L, $I = 0.01$ M $NaNO_3$, $T = 298$ K, [U(VI)] = 40 mg/L, $P_{CO_2} = 3.8 \times 10^{-4}$ atm

obtained on a Philips X'Pert Pro Panalytical diffractometer equipped. Thermogravimetric analysis (TGA) of the samples were recorded on a TA Q50 DTA/TGA apparatus (USA). Scanning electron microscopy (SEM) were obtained using an S-4800 (Hitachi) microscope.

Results and discussion

Adsorption behavior studies

Effect of pH

The species of U(VI) and the surface charge of the amidoxime-based activated carbon can be affected by pH, therefore, study the effect of pH is of great significance for U(VI) adsorption [21]. As shown in Fig. 2a, the adsorption percentage of U(VI) on activated carbon and amidoxime-based activated carbon increased with pH increasing from 2.5 to 6.0, whereas the adsorption percentage of U(VI) adsorbed on activated carbon and amidoxime-based activated carbon decrease with pH further increasing, indicated that the adsorption is pH dependent. At lower pH, the protonation of the amidoxime on amidoxime-based activated carbon and the competition between U(VI) and H^+ limited the adsorption process. With the increase of pH, the number of H^+ diminished and the protonation became weak, the adsorption percentage increased gradually. Figure 2b describes the species distribution of U(VI) depend on the pH values. At pH < 5.0, UO_2^{2+} was the main existing species of U(VI). As the pH increased (pH > 5.0), hydrolysis of U(VI) increased and formed different hydroxy complexes. At 5.0 < pH < 7.0,

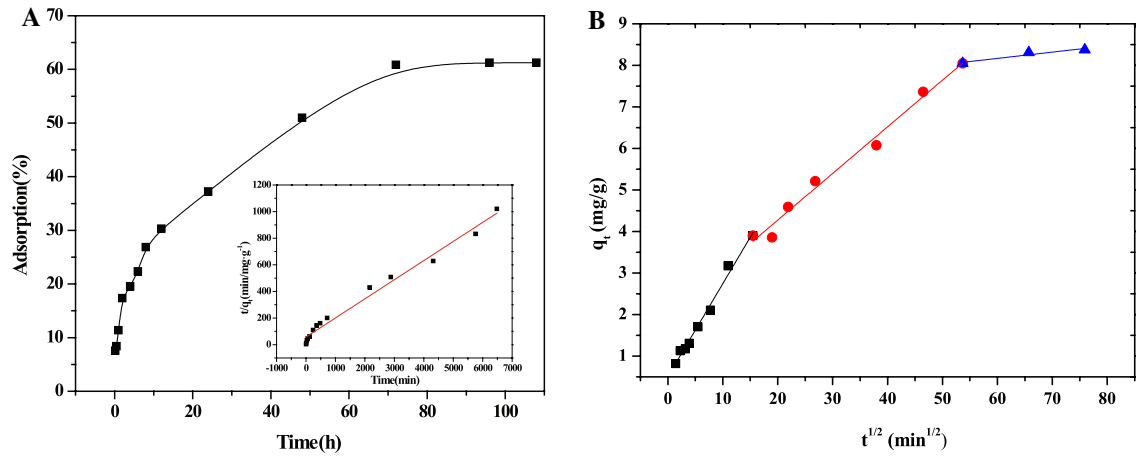

Fig. 2 Effect of contact time on the adsorption of U(VI) onto **a** amidoxime-based activated carbon (bottom right:the fitting plot of the pseudo-second-order equation); **b** Weber–Morris model. pH = 5.00, $m/V = 3.6$ g/L, $I = 0.01$ M $NaNO_3$, $T = 298$ K, [U(VI)] = 40 mg/L

the dominant species was $(UO_2)_3(OH)_5^+$ and $(UO_2)_4(OH)_7^+$. A further increase in pH value will generate negatively charged species, including $UO_2(CO_3)_2^{2-}$ and $UO_2(CO_3)_3^{4-}$, the hydrolysate of U(VI) is not favored by the amidoxime-based activated carbon [22], the adsorption percentage declined with the increasing of pH. Furthermore, the adsorption percentage of U(VI) adsorbed on amidoxime-based activated carbon is remarkably higher than that of U(VI) on activated carbon, this is due to that the surface groups of amidoxime-based activated carbon are favorable for binding U(VI) [23], amidoxime-based activated carbon can be an alternative material for uranium recovery from waste liquid (Fig. 1).

Effect of contact time and adsorption kinetics

The contact time of adsorbent and adsorbate is one of the most significant influence factor that could control the adsorption percentage [24]. Effect of contact time on the adsorption towards U(VI) by amidoxime-based activated carbon was conducted at pH 5.0 and the result was shown in Fig. 2. The fitted results of pseudo-first-order, pseudo-second-order and Weber–Morris model were summarized in Tables 1 and 2. As shown in Table 1, the pseudo-second-order model fitted better than the pseudo-first-order model due to the higher regression coefficient (R^2) value (0.9830) and less difference of calculated q_e (8.69 mg/g) with experimental adsorption capacity (8.71 mg/g). The adsorption kinetic of U(VI) on amidoxime-based activated carbon implied that chemical complexing reaction dominated the adsorption process [25]. Compared to conventional amidoxime resins and fibers, the same conclusion was obtained [27, 27, 28]. The Weber–Morris model indicated that the adsorption process of U(VI) on amidoxime-based activated carbon involves three steps (Fig. 2b). The obtained parameters are listed in Table 2, where K_{ad} (K_{ad1}, K_{ad2}, K_{ad3}) is the rate constants of the adsorption three steps, C is the intercept of the line. The first step is the external transfer step, the second step suggests the intra-particle diffusion process, the final stage corresponding to the final equilibrium step [29]. The intra-particle diffusion process is the rate limiting step in the U(VI) adsorption onto amidoxime-based activated carbon process.

Table 1 Kinetic parameters of pseudo-first-order and pseudo-second-order models

Pseudo-first-order model		Pseudo-second-order model	
k_1 (g/mg min)	8.94	k_2 (g/mg min)	5.91×10^{-4}
q_e (mg/g)	4.13	q_e (mg/g)	8.69
R^2	0.8180	R^2	0.9830

Adsorption isotherm analysis

The initial concentration of U(VI) is another important influence factor for the interaction between amidoxime-based activated carbon and U(VI) [30]. Figure 3 shows the effects of U(VI) initial concentration on the adsorption to amidoxime-based activated carbon. The experimental data were fitted by the following three types of isotherms, the results were shown in Fig. 4. The Langmuir isotherm can be expressed [31]:

$$\frac{C_e}{q_e} = \frac{C_e}{q_m} + \frac{1}{K_L q_m} \tag{3}$$

The Freundlich isotherm is given as [32]:

$$lnq_e = lnK_F + \frac{1}{m} lnC_e \tag{4}$$

where K_F is the constant related to the adsorption capacity, and n is the Freundlich constant.

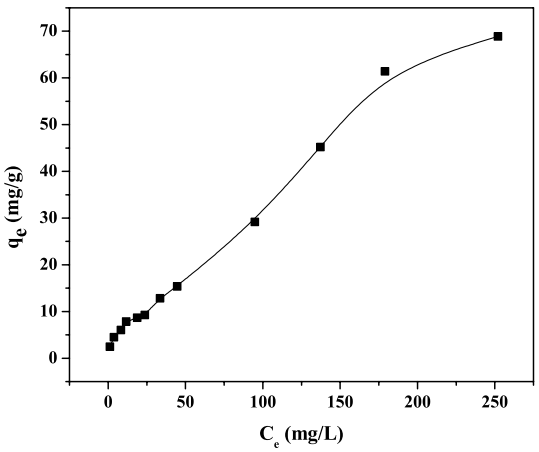

Fig. 3 Effect of initial concentration of U(VI) on the adsorption on amidoxime-based activated carbon. pH = 5.00, m/V = 3.6 g/L, I = 0.01 M $NaNO_3$, T = 298 K

Table 2 Kinetic parameters of the Weber–Morris model

First stage		Second stage		Third stage	
k_{ad1} (g/mg min)	0.22	k_{ad2} (g/mg min)	0.11	k_{ad3} (g/mg min)	0.02
C_1 (μg/g)	0.50	C_2 (μg/g)	1.91	C_3 (μg/g)	7.26
R_1^2	0.9874	R_2^2	0.9830	R_3^2	0.9240

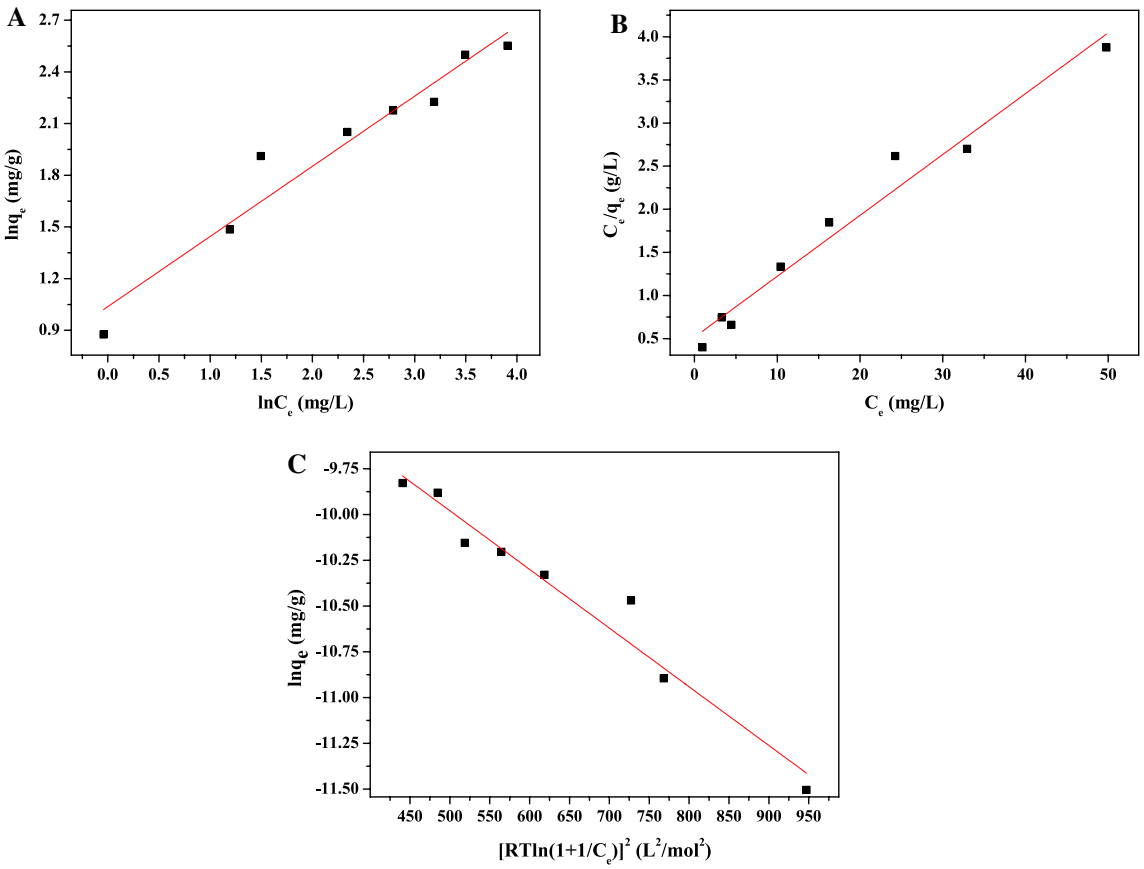

Fig. 4 The adsorption isotherms of U(VI) onto amidoxime-based activated carbon. **a** Freundlich isotherm; **b** Langmuir isotherm; **c** D–R isotherm

The D–R isotherm assumed that the adsorbent has a heterogeneous adsorption energy [33]. The model can be expressed [34]:

$$lnq_e = lnq_k - B\eta^2 \tag{5}$$

$$\eta = RTln\left(1 + \frac{1}{c_e}\right) \tag{6}$$

$$E = \frac{1}{\sqrt{2B}} \tag{7}$$

where B (mol^2/kJ^2) is the D–R constant, q_k (mol/g) is the D–R adsorption capacity, ε is the Polanyi potential, and E (kJ/mol) is the free energy change.

The fitting results are summarized in Table 3. Upon comparing the linear regression coefficiencies (R^2), the U(VI) adsorption was better simulated by Langmuir model, which suggested that U(VI) adsorption onto the amidoxime-based activated carbon obeys the Langmuir isotherm model. The Langmuir isotherm was commonly used to describe homogeneous adsorption that all the absorption sites on a homogeneous surface having equal adsorbate affinity, thus, the adsorption process of amidoxime-based activated carbon for U(VI) was considered

Table 3 Adsorption isotherm parameters of U(VI) adsorption onto amidoxime-based activated carbon

Model	Freundlich model		Langmuir model		D-R model	
Parameter	n	2.46	q_{max} (mg/g)	14.16	B (mol^2/kJ^2)	0.0032
	K_F (L/g)	2.82	K_L (L/mg)	0.14	q_k (mg/g)	2.30×10^{-4}
	R^2	0.9388	R^2	0.9666	E (kJ/mol)	12.48
					R^2	0.9533

homogeneous and a monolayer process. Other research about U(VI) adsorption on amidoxime-based adsorbent got the same conclusion [27, 35, 36]. The q_{max} of Langmuir isotherm model is the maximum adsorption capacity, the q_{max} value of U(VI) adsorbed on amidoxime-based activated carbon was calculated to be 14.16 mg/g. The nature of adsorption process can be physical for the $E < 8$ kJ/mol or chemical for $8 < E < 16$ kJ/mol, as shown in Table 3, the value of E indicating that the adsorption process is controlled by chemical adsorption [37–39].

Temperature and thermodynamic parameters

At 298, 308, 318, 328 and 338 K, the thermodynamic parameters of U(VI) adsorbed onto amidoxime-based activated carbon composites were calculated using the Van't Hoff equation [7].

Table 4 showed the calculated the thermodynamic parameters. The results indicated that the adsorption on amidoxime-based activated carbon is spontaneous and endothermic [40, 41]. Xie et al. [27] reported that the adsorption of uranium(VI) onto amidoxime-functionalized fibers, the results showed that the adsorption is spontaneous and endothermic process. Heshmati et al. [28] got the same conclusion that adsorption of U(VI) on PAO chelating resin is endothermic and a feasible process.

Effect of adsorbent dosage

Adsorbent dosage determines the number of available binding sites and the dosage of amidoxime-based activated carbon will affect the adsorption capacity. The effect of adsorbent dose on U(VI) adsorption was represented in Fig. 5, it was clear that the adsorption capacity of U(VI) increased sharply from 5 to 95% at amidoxime-based activated carbon dose increase from 0.02 to 7 g/L. This may be attributed to there was more available adsorption sites in the solution with increasing the adsorbent dosage [9].

Table 4 Thermodynamic parameters for U(VI) adsorption onto amidoxime-based activated carbon

T (K)	ΔH (kJ/mol)	ΔS (J/mol K)	ΔG (kJ/mol)	R^2
298	14.72	51.95	− 0.58	0.9502
308		− 1.49	− 0.58	
318		− 1.81	− 0.58	
328		− 2.40	− 0.58	
338		− 2.69	− 0.58	

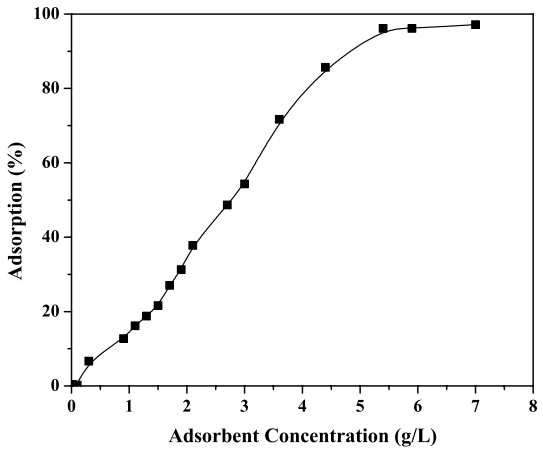

Fig. 5 Effect of adsorbent dosage on the adsorption of U(VI) onto amidoxime-based activated carbon. pH = 5.00, I = 0.01 M $NaNO_3$, T = 298 K, [U(VI)] = 40 mg/L

Characterization analysis

Elemental analysis

To further confirm the carbon, nitrogen, and hydrogen contents in the activated carbon and amidoxime-based activated carbon, elemental analysis was carried out. According to the results shown in Table 5, negligible nitrogen content was detected for the activated carbon, it could be attributed to N-containing impurities in the activated carbon. In comparison with the activated carbon, an obvious increase of nitrogen content was observed for amidoxime-based activated carbon. This indicated that amidoxim groups were grafted onto activated carbon.

FT-IR analysis

FT-IR analysis was further carried out to verify the conversion of functional group in the reaction process. As shown in Fig. 6, after modification, several peaks appeared in the spectrum compared with that of activated carbon. Peaks at 1639 cm^{-1} could be ascribed to the stretching vibration of C = N, the peaks at 1360 cm^{-1} could be assigned to the bending vibration of NH_2, the peaks at 900 cm^{-1} could be ascribed to the stretching vibration of the N–O in the amidoxime group.

Table 5 Elemental analysis results for the activated carbon and amidoxime-based

Sample	C wt%	N wt%
Activated carbon	90.48	0.18
Amidoximebased activated carbon	72.54	5.26

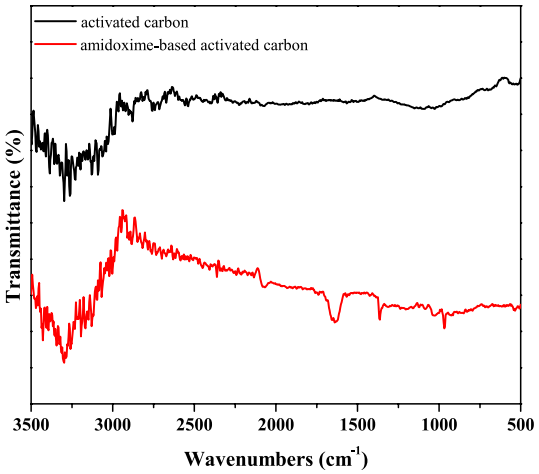

Fig. 6 FT-IR spectra of activated carbon and amidoxime-based activated carbon

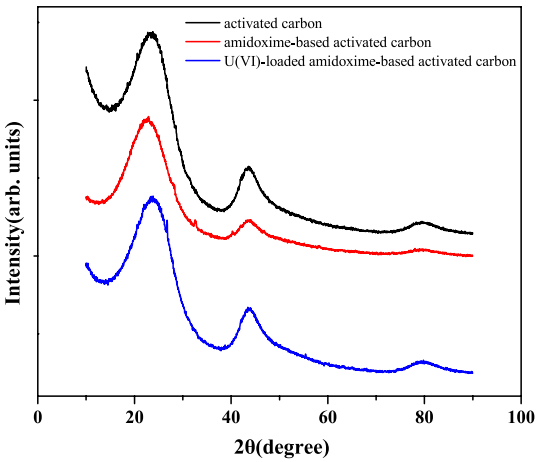

Fig. 7 XRD diffraction patterns of activated carbon and amidoxime-based activated carbon

The results suggest that the amidoxime groups were grafte onto activated carbon successfully.

XRD analysis

XRD patterns of activated carbon and amidoxime-based activated carbon are shown in Fig. 7. As evident, the XRD patterns of amidoxime-based activated carbon do not show obvious fresh peaks compared with activated carbon, which indicates that the amidoxime-based activated carbon maintain the original structures of activated carbon.

N_2 adsorption-desorption isotherm

The N_2 adsorption-desorption isotherms of activated carbon and amidoxime-based activated carbon are shown in Fig. 8. The Brunauer–Emmett Teller (BET) surface area of activated carbon and amidoxime-based activated carbon were calculated to be 646.77 and 357.17 m^2/g^{-1}, respectively. The BET surface area of amidoxime-based activated carbon became smaller after modification, it means that the pores of activated carbon were partially blocked after modification.

Thermogravimetric analysis

Thermogravimetric analysis is favourable for analyze the thermal behaviors of activated carbon and amidoxime-based activated carbon. As shown in Fig. 9, bare activated carbon is the most stable sample. For amidoxime-based activated carbon, the first process occurs at 100 °C attributes to the elimination of physically adsorbed moisture on the surface of the particles [42]; the second process occurs from 100 to 400 °C, which can be assigned to thermal decomposition of organic components; the third process occurs from 400 to 700 °C, which is caused by carbon

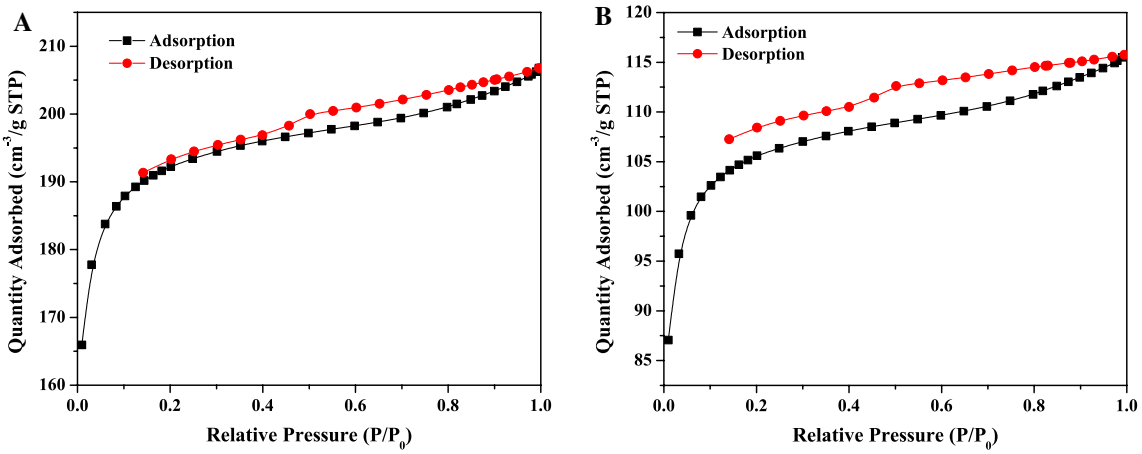

Fig. 8 Nitrogen adsorption-desorption isotherm of activated carbon (**a**) and amidoxime-based activated carbon (**b**)

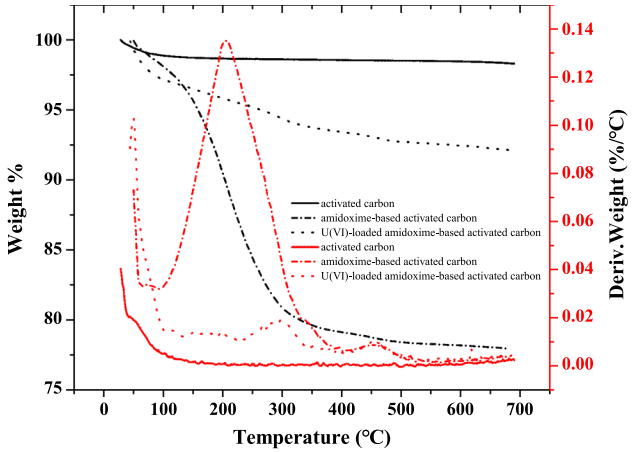

Fig. 9 Thermogravimetric analysis of activated carbon and amidoxime-based activated carbon

chain combustion in activated carbon. As for U(VI)-loaded amidoxime-based activated carbon, the thermal decomposition was relatively gentle, however, the weight loss was lower than that of the bare amidoxime-based activated carbon. This was because of the adsorption of U(VI) on the surface of amidoxime-based activated carbon [43].

Scanning electron microscopy (SEM) analysis

The surface morphologies changes before and after activated carbon modified by amidoxime were analyzed via SEM. As shown in Fig. 10, after modification, the surface of amidoxime-based artificial was much rougher than activated carbon. Figure 10e, f showed the SEM image of amidoxime-based activated carbon after U(VI) adsorption. The surface of amidoxime-based activated carbon became rougher, a remarkable amount of particles were disposed on amidoxime-based activated carbon surface, which demonstrated that U(VI) was adsorbed onto the surface of amidoxime-based activated carbon.

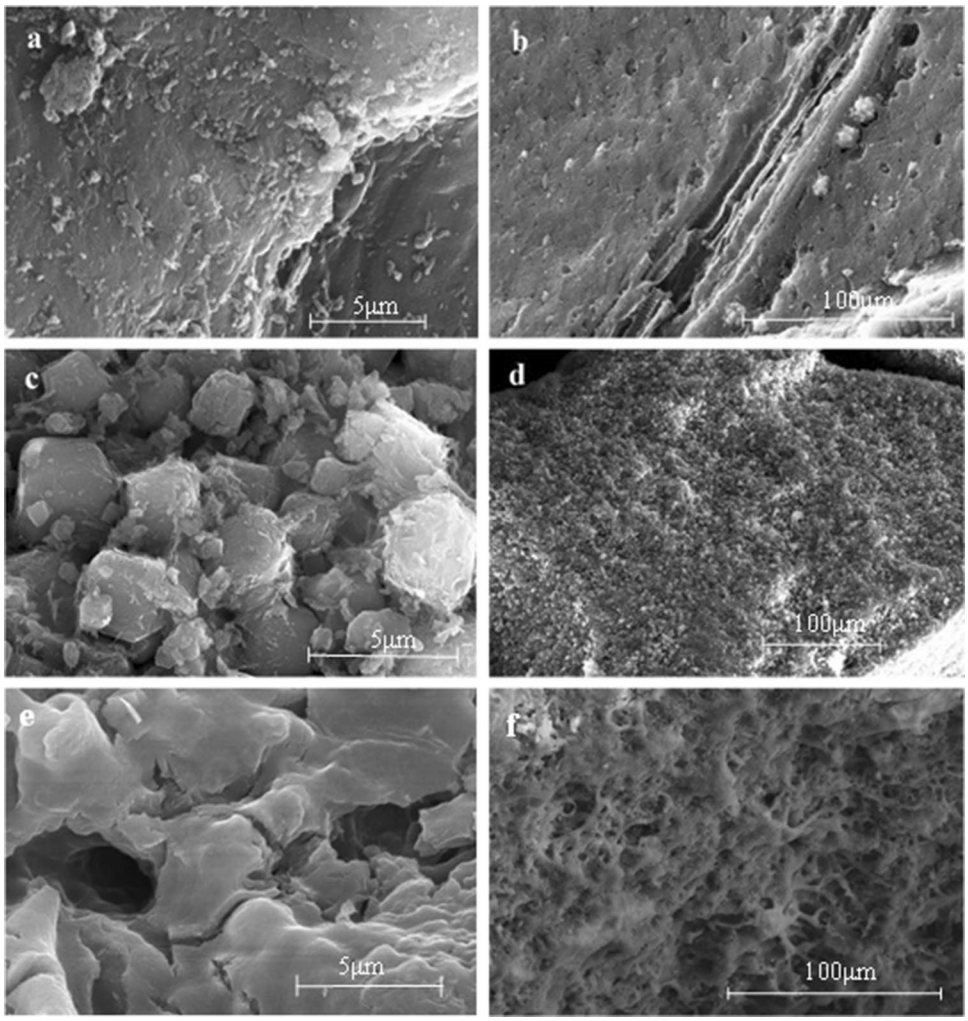

Fig. 10 SEM images of **a**, **b** activated carbon; **c**, **d** amidoxime-based activated carbon; **e**, **f** U(VI)-loaded amidoxime-based activated carbon

Conclusions

The amidoxime-based activated carbon was prepared for study the adsorption process of U(VI). The adsorption data of U(VI) adsorption onto amidoxime-based activated carbon can be described by Langmuir isotherm. The consequence of experimental indicated that amidoxime-based activated carbon had a high removal amount towards U(VI), which was much higher than that of activated carbon, the synthesis of amidoxime-based activated carbon could offer a promising opportunities for further improvements in removal ofU(VI).

Acknowledgements The authors gratefully acknowledge support from the Foundation of Heilongjiang Postdoctoral Science Foundation (LBH-Z17050), the China Postdoctoral Science Foundation (2019M651257), the National Natural Science Foundation of China (21771045), the Fundamental Research Funds for the Central Universities (3072019CFJ1501), and the Decommissioning of Nuclear Facilities and special funds for radioactive waste management ([2017]955). And the authors acknowledged the Innovation Center of Nuclear Materials for National Defense Industry.

Compliance with ethical standards

Conflicts of interest The authors declare that they have no conflict of interest.

References

1. Wu F, Pu N, Ye G, Sun T, Wang Z, Song Y, Wang W, Huo X, Lu Y, Chen J (2017) Performance and mechanism of uranium adsorption from seawater to poly(dopamine)-inspired sorbents. Environ Sci Technol 51(8):4606–4614
2. Xiao J, Jing Y, Yao Y, Wang X, Jia Y (2019) Synthesis of amidoxime-decorated 3d cubic mesoporous silica via self-assembly co-condensation as a superior uranium(VI) adsorbent. J Mol Liq 277:843–855
3. Wang D, Xu Y, Xiao D, Qiao Q, Yin P, Yang Z, Li J, Winchester W, Wang Z, Hayat T (2019) Ultra-thin iron phosphate nanosheets for high efficient U(VI) adsorption. J Hazard Mater 371:83–93
4. Wang Y, Huang H, Duan S, Liu X, Sun J, Hayat T, Alsaedi A, Li J (2017) A new application of a mesoporous hybrid of tungsten oxide and carbon as an adsorbent for elimination of Sr^{2+} and Co^{2+} from an aquatic environment. ACS Sustain Chem Eng 6(2):2462–2473
5. Zhao Y, Wang X, Li J, Wang X (2015) Amidoxime functionalization of mesoporous silica and its high removal of U(VI). Polym Chem 6(30):5376–5384
6. Yuan D, Chen L, Xiong X, Yuan L, Liao S, Wang Y (2016) Removal of uranium(VI) from aqueous solution by amidoxime functionalized superparamagnetic polymer microspheres prepared by a controlled radical polymerization in the presence of DPE. Chem Eng J 285:358–367
7. Zhang M, Gao Q, Yang C, Pang L, Wang H, Li H, Li R, Xu L, Xing Z, Hu J et al (2016) Preparation of amidoxime-based nylon-66 fibers for removing uranium from low-concentration aqueous solutions and simulated nuclear industry effluents. Ind Eng Chem Res 55(40):10523–10532
8. Zhao C, Liu J, Yuan G, Liu J, Zhang H, Yang J, Yang Y, Liu N, Sun Q, Liao J (2018) A novel activated sludge-graphene oxide composites for the removal of uranium(VI) from aqueous solutions. J Mol Liq 271:786–794
9. Fan Qh, Li P, Yf Chen, Ws Wu (2011) Preparation and application of attapulgite/iron oxide magnetic composites for the removal of U(VI) from aqueous solution. J Hazard Mater 192(3):1851–1859
10. Zhao G, Huang X, Tang Z, Huang Q, Niu F, Wang X (2018) Polymer-based nanocomposites for heavy metal ions removal from aqueous solution: a review. Polym Chem 9(26):3562–3582
11. Yin L, Song S, Wang X, Niu F, Ma R, Yu S, Wen T, Chen Y, Hayat T, Alsaedi A et al (2018) Rationally designed core-shell and yolk-shell magnetic titanate nanosheets for efficient U(VI) adsorption performance. Environ Pollut 238:725–738
12. Bq Lu, Li M, Xw Zhang, Huang Cm Wu, Xy Fang Q (2018) Immobilization of uranium into magnetite from aqueous solution by electrodepositing approach. J Hazard Mater 343:255–265
13. Dutta DP, Nath S (2018) Low cost synthesis of SiO_2/ C nanocomposite from corn cobs and its adsorption of uranium(VI), chromium(VI) and cationic dyes from wastewater. J Mol Liq 269:140–151
14. Ma D, Hu S, Li Y, Xu Z (2019) Adsorption of uranium on phosphoricacid-activated peanut shells. Sep Sci Technol. https://doi.org/10.1080/01496395.2019.1606016
15. Zhao Y, Liu C, Feng M, Chen Z, Li S, Tian G, Wang L, Huang J, Li S (2010) Solid phase extraction of uranium(VI) onto benzoylthiourea-anchored activated carbon. J Hazard Mater 176(1–3):119–124
16. Starvin A, Rao TP (2004) Solid phase extractive preconcentration of uranium(VI) onto diarylazobisphenol modified activated carbon. Talanta 63(2):225–232
17. Saleh TA, Tuzen M, Sarı A et al (2017) Polyethylenimine modified activated carbon as novel magnetic adsorbent for the removal of uranium from aqueous solution. Chem Eng Res Des 117:218–227
18. Xie L, Wang Y, Wang Y, Li X, Tian Q, Liu D, Sun G, Wang X (2018) Study of poly(acrylamidoxime) brushes conformation with uranium adsorption by neutron reflectivity. Mater Lett 220:47–49
19. Ladshaw AP, Wiechert AI, Das S, Yiacoumi S, Tsouris C (2017) Amidoxime polymers for uranium adsorption: influence of comonomers and temperature. Materials 10(11):1268
20. Bai J, Yao H, Fan F, Lin M, Zhang L, Ding H, Lei F, Wu X, Li X, Guo J et al (2010) Biosorption of uranium by chemically modified rhodotorula glutinis. J Environ Radioact 101(11):969–973
21. Wang Y, Wang Z, Ang R, Yang J, Liu N, Liao J, Yang Y, Tang J (2015) Synthesis of amidoximated graphene oxide nanoribbons from unzipping of multiwalled carbon nanotubes for selective separation of uranium(VI). RSC Adv 5(108):89309–89318
22. Wang X, Ji G, Zhu G, Song C, Zhang H, Gao C (2019) Surface hydroxylation of SBA-15 via alkaline for efficient amidoxime-functionalization and enhanced uranium adsorption. Sep Purif Technol 209:623–635
23. Zhang Z, Dong Z, Wang X, Ying D, Niu F, Cao X, Wang Y, Hua R, Liu Y, Wang X (2018) Ordered mesoporous polymer-carbon composites containing amidoxime groups for uranium removal from aqueous solutions. Chem Eng J 341:208–217
24. Aljarrah M, Al-Harahsheh MS, Mayyas M, Alrebaki M (2018) In situ synthesis of quaternary ammonium on silica-coated magnetic nanoparticles and it's application for the removal of uranium(VI) from aqueous media. J Environ Chem Eng 6(5):5662–5669
25. Li W, Liu Q, Liu J, Zhang H, Li R, Li Z, Jing X, Wang J (2017) Removal U(VI) from artificial seawater using facilely and covalently grafted polyacrylonitrile fibers with lysine. Appl Surf Sci 403:378–388

26. Ma F, Dong B, Gui Y, Cao M, Han L, Jiao C, Lv H, Hou J, Xue Y (2018) Adsorption of low-concentration uranyl ion by amidoxime polyacrylonitrile fibers. Ind Eng Chem Res 57(51):17384–17393
27. Xie CY, Jing SP, Wang Y, Lin X, Bao HL, Guan CZ, Jin C, Wang JQ (2017) Adsorption of uranium(VI) onto amidoxime-functionalized ultra-high molecular weight polyethylene fibers from aqueous solution. Nucl Sci Technol 28(7):94
28. Heshmati H, Torab-Mostaedi M, Ghanadzadeh Gilani H, Heydari A (2015) Kinetic, isotherm, and thermodynamic investigations of uranium(VI) adsorption on synthesized ion-exchange chelating resin and prediction with an artificial neural network. Desalination Water Treat 55(4):1076–1087
29. Tran HN, You SJ, Hosseini-Bandegharaei A, Chao HP (2017) Mistakes and inconsistencies regarding adsorption of contaminants from aqueous solutions: a critical review. Water Res 120:88–116
30. Wei X, Liu Q, Zhang H, Liu J, Chen R, Li R, Li Z, Liu P, Wang J (2018) Rapid and efficient uranium(VI) capture by phytic acid/polyaniline/FeOOH composites. J Colloid Interface Sci 511:1–11
31. Guibal E, Milot C, Tobin JM (1998) Metal-anion sorption by chitosan beads: equilibrium and kinetic studies. Ind Eng Chem Res 37(4):1454–1463
32. Freundlich H (1907) Über die adsorption in lösungen. Z Phys Chem 57(1):385–470
33. Yang P, Liu Q, Liu J, Chen R, Li R, Bai X, Wang J (2019) Highly efficient immobilization of uranium(VI) from aqueous solution by phosphonate-functionalized dendritic fibrous nanosilica (DFNS). J Hazard Mater 363:248–257
34. Dabrowski A (2001) Adsorption-from theory to practice. Adv Colloid Interface Sci 93(1–3):135–224
35. Yin Z, Xiong J, Chen M, Hu S, Cheng H (2016) Recovery of uranium(VI) from aqueous solution by amidoxime functionalized wool fibers. J Radioanal Nucl Chem 307(2):1471–1479
36. Hazer O, Kartal Ş (2010) Use of amidoximated hydrogel for removal and recovery of U(VI) ion from water samples. Talanta 82(5):1974–1979
37. Duan S, Xu X, Liu X, Wang Y, Hayat T, Alsaedi A, Meng Y, Li J (2018) Highly enhanced adsorption performance of U(VI) by non-thermal plasma modified magnetic Fe_3O_4 nanoparticles. J Colloid Interface Sci 513:92–103
38. Imam EA, El-Sayed IET, Mahfouz MG, Tolba AA, Akashi T, Galhoum AA, Guibal E (2018) Synthesis of α-aminophosphonate functionalized chitosan sorbents: effect of methyl vs phenyl group on uranium sorption. Chem Eng J 352:1022–1034
39. Zhang Z, Duan S, Chen H, Zhang F, Hayat T, Alsaedi A, Li J (2018) Synthesis of porous magnetic $Ni_{0.6}Fe_{2.4}O_4$ nanorods for highly efficient adsorption of U(VI). J Chem Eng Data 63(5):1810–1820
40. Li P, Wang J, Wang X, He B, Pan D, Liang J, Wang F, Fan Q (2018) Arsenazo-functionalized magnetic carbon composite for uranium(VI) removal from aqueous solution. J Mol Liq 269:441–449
41. Yang P, Zhang H, Liu Q, Liu J, Chen R, Yu J, Hou J, Bai X, Wang J (2019) Nano-sized architectural design of multi-activity graphene oxide (GO) by chemical post-decoration for efficient uranium(VI) extraction. J Hazard Mater 375:320–329
42. Sun Y, Shao D, Chen C, Yang S, Wang X (2013) Highly efficient enrichment of radionuclides on graphene oxide-supported polyaniline. Environ Sci Technol 47(17):9904–9910
43. Nakkeeran E, Selvaraju N (2017) Biosorption of chromium(VI) in aqueous solutions by chemically modified strychnine tree fruit shell. Int J Phytorem 19(12):1065–1076